The synthesis and exchange bias effect of monodisperse NiO nanocrystals*

Duan Han-Ning(段寒凝), Yuan Song-Liu(袁松柳)†,
Zheng Xian-Feng(郑先锋), and Tian Zhao-Ming(田召明)

School of Physics, Huazhong University of Science and Technology, Wuhan 430074, *China*

(Received 23 November 2011; revised manuscript received 19 December 2011)

Monodisperse NiO nanocrystals with an average particle size of 3 ± 0.4 nm are successfully synthesized by the thermal decomposition of Ni-oleylamine complex in an organic solvent under a continuous O_2 flux. The crystalline structure and the morphology of the product are investigated by X-ray diffraction, X-ray photoelectron spectroscopy, and transmission electron microscopy. Magnetization and alternating-current (ac) susceptibility measurements indicate that the structure of the particles can be considered as consisting of an antiferromagnetically ordered core and a spin-glass-like surface shell. In addition, both the exchange bias field and the vertical magnetization shift can be observed in this system at 10 K after field cooling. This observed exchange bias effect is explained in terms of the exchange interaction between the antiferromagnetic core and the spin-glass-like shell.

Keywords: nanocrystalline materials, antiferromagnetics, spin glass, exchange bias

PACS: 81.07.Bc, 75.50.Ee, 75.50.Lk, 75.30.Et **DOI:** 10.1088/1674-1056/21/7/078101

1. Introduction

A magnetic system containing a ferromagnetic/antiferromagnetic (FM/AFM) interface may exhibit the exchange bias (EB) effect,[1−5] which is typically characterized by an enhanced coercivity and a field shift in the hysteresis loop due to the interaction at the interface between FM and AFM after the system has been cooled down through the critical temperature in an external magnetic field. This phenomenon was first discovered in 1956 by Meiklejohn and Bean[6] when studying Co particles coated with a layer of AFM CoO. In the past two decades, the study of the EB effect has mainly focused on FM/AFM nanocomposite systems, such as Ni/NiO, Fe_3O_4/FeO, and $CoCr_2O_4/Cr_2O_3$,[7−9] because it has been shown that the FM/AFM exchange interaction can be useful in overcoming the superparamagnetic limit and increasing the thermoremanence of FM nanoparticles,[10] a critical bottleneck for magnetic data storage applications. Besides, the EB effect can also be observed in the single-phase compound. The observation of the shift of the magnetic hysteresis loop in $NiFe_2O_4$ nanoparticles prepared by the ball-milled method at low temperature was reported by Kodama and Berkowitz,[11] and the EB was ascribed to the exchange coupling of ferrimagnetically aligned core spins and a spin-glass-like (SGL) surface layer. Simultaneously, Kodama *et al.*[12] found that the AFM NiO nanoparticles exhibit a large loop shift and a vertical magnetization shift at low temperature, where the exchange coupling between the frozen moments associated with uncompensated surface spins and the AFM core plays an important role. However, there are no reports on the synthesis and the EB effect of monodisperse NiO nanocrystals with sizes less than 5 nm. Therefore, it would be of interest to investigate the microstructure and the EB effect of very small NiO nanocrystals.

NiO is used for a variety of applications, such as catalysts, magnetic materials, electrochromic films, gas sensors, and fuel cell electrodes.[13−17] Therefore, many methods have been used to synthesize NiO. Among the chemical methods, the thermal decomposition of organometallic compounds in high-boiling-point inert organic solvents has been proven to be an attractive route for the synthesis of monodisperse nanocrystals with high yield, narrow size distribution, and good crystallinity.[18] In the present paper, monodisperse NiO nanocrystals with an average particle size of 3 ± 0.4 nm are synthesized via a modified thermal decomposition route. Compared with

*Project supported by the National Natural Science Foundation of China (Grant No. 11174092).
†Corresponding author. E-mail: yuansl@hust.edu.cn
© 2012 Chinese Physical Society and IOP Publishing Ltd

the conventional thermal decomposition procedures, which are carried out under Ar atmosphere, the current synthetic procedure is a modified version under a continuous O_2 flux. The SGL behavior and the EB effect have also been observed at low temperatures in monodisperse NiO nanocrystals.

2. Experiment

All the materials used were purchased without further purification. The chemical reactions were carried out in a mild temperature organic solution under O_2 atmosphere. The overall synthetic procedure is shown in Fig. 1. In a typical synthesis route, a mixture of oleylamine (11 g, 96%) and nickel(acetylacetonate)$_2$ (0.52 g, 99%) was stirred magnetically at 100 °C to obtain the Ni-oleylamine complex. The resulting green solution was injected with triphenylphosphine (3.7 g, 99%), and was heated up to 200 °C for 30 min. After cooling to room temperature naturally, excess ethanol was added to the yellowish-brown solution to give a yellow precipitate, which was isolated via centrifugation, washed fully with ethanol, and dried before dispersing in hexane.

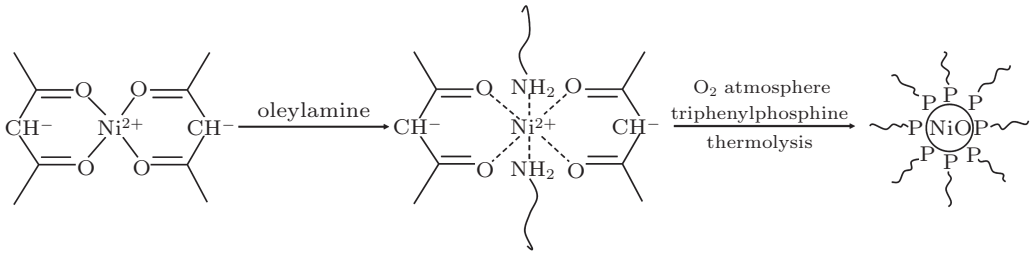


Fig. 1. The synthesis of NiO nanocrystals by the thermal decomposition of Ni-oleylamine complex under O_2 atmosphere.

The structure and morphology of the as-synthesized nanocrystals were characterized using X-ray diffraction (XRD, Philips X'pert pro) and transmission electron microscopy (TEM, FEI Tecnai G2). X-ray photoelectron spectroscopy (XPS, PHI Quantera SXM) was used to determine the oxidation state of Ni in the NiO nanocrystal. Magnetic measurements were performed using a commercial physical property measurement system (PPMS, Quantum Design).

3. Results and discussion

The XRD pattern for the NiO nanocrystal is shown in Fig. 2. The diffraction peaks observed at the angles of 37.4°, 43.5°, 62.9°, 75.3°, and 79.3° can be indexed to the (111), (200), (220), (311), and (222) planes of the cubic NiO phase, respectively. The calculated lattice parameter of the NiO nanocrystal is $a = 4.178$ Å, which is in good agreement with the value of 4.172 Å reported in the literature (JCDF card No. 78-0423). Notably, no other impurity phase is observed in the XRD pattern.

Figure 3(a) shows a TEM image at low magnification, revealing that the NiO nanocrystals have a tight size distribution with an average particle diameter of 3 ± 0.4 nm. The single crystallinity of the particle is checked by the high-resolution TEM (HRTEM) images. We show a HRTEM image of a typical single particle in Fig. 3(b), which indicates the crystalline nature in the core part and the presence of structure disordered layers in the surface part of the nanocrystal. The lattice spacing of 0.208 nm in the image corresponds to the interplanar separation between the (200) lattice planes. Although the mechanism for the formation of the structural disorder regions is not clear yet, it can be correlated with the broken chemical bond and the amorphous structural defects, which extend to a few atomic layers from the surface of AFM NiO nanocrystals.[19] Figure 3(c) shows the selected area

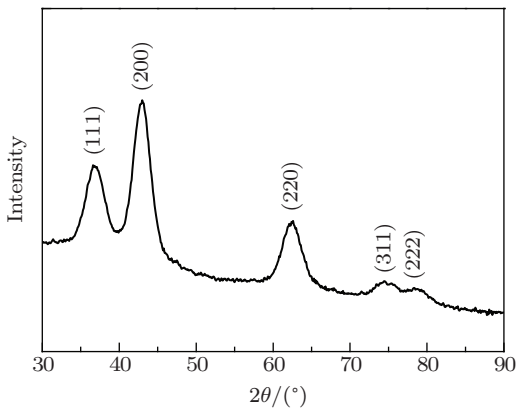


Fig. 2. The XRD pattern of the monodisperse NiO nanocrystals.

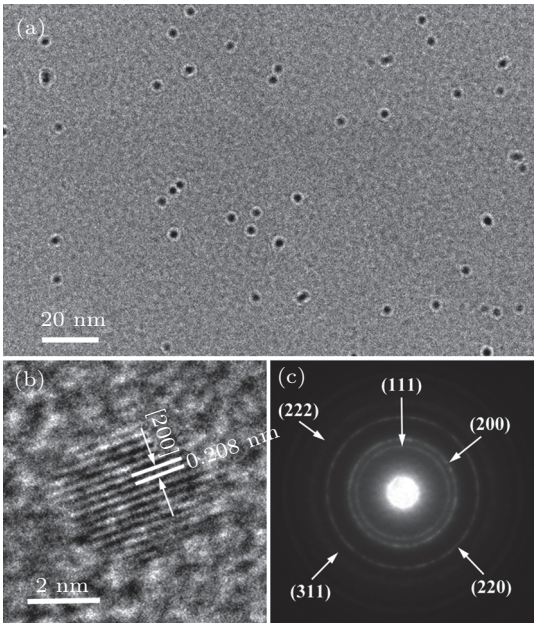


Fig. 3. (a) Typical TEM image, (b) HRTEM image of a single nanocrystal, and (c) the corresponding SAED pattern of the NiO nanocrystals.

electron diffraction (SAED) pattern taken from the same area of the TEM image in Fig. 3(a), which confirms that the lattice spacings are consistent with those found in NiO. This is consistent with the XRD data given in Fig. 2.

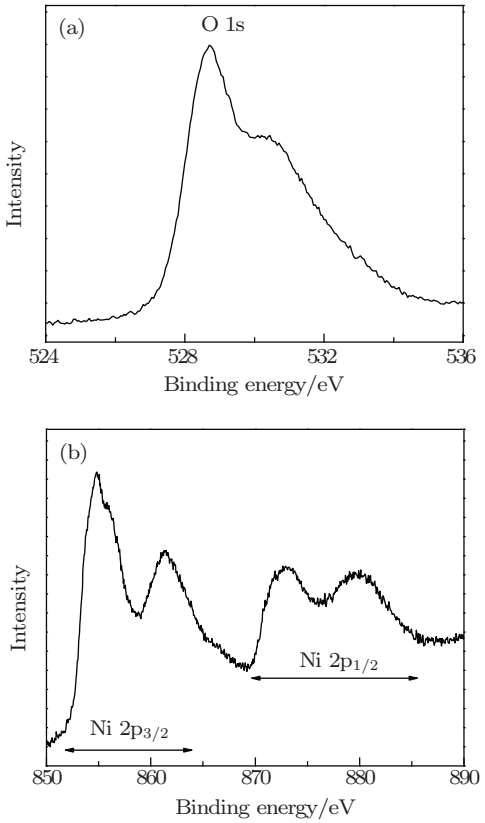


Fig. 4. The XPS spectra for the (a) O 1s and (b) Ni 2p core levels of the monodisperse NiO nanocrystals.

Further evidence for the purity and the composition of the products is obtained by XPS. Figures 4(a) and 4(b) show the XPS spectra of the nanocrystals for the O 1s and Ni 2p core levels, respectively. The O 1s spectrum consists of a main peak at 529.5 eV with a shoulder at ~ 1 eV higher than the binding energy. The Ni 2p spectrum comprises two regions representing the Ni $2p_{3/2}$ (850–865 eV) and the Ni $2p_{1/2}$ (870–885 eV) spin-orbit levels. The Ni $2p_{3/2}$ region consists of a main peak at 854.8 eV with a shoulder peak ($\sim$ 1 eV above the main peak) and a satellite peak ($\sim$ 7 eV above the main peak); similar features are observed for the $2p_{1/2}$ region. The binding energies of the main and the satellite peaks in the O 1s and the Ni 2p core levels are consistent with those obtained in the previous report on NiO.[20]

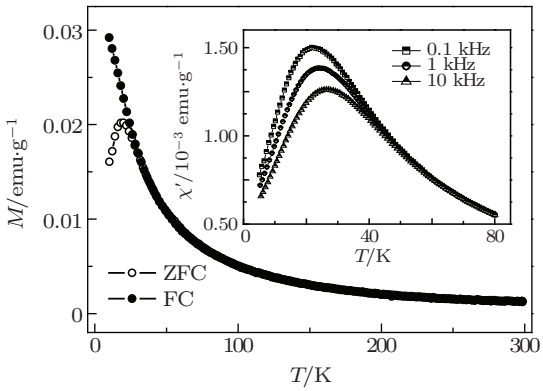


Fig. 5. Temperature dependences of magnetization in ZFC and FC processes. The magnetic field used is 0.01 T. The inset shows the temperature dependences of the real component of ac magnetic susceptibility under different frequencies.

The temperature-dependent magnetization curves in the zero-field-cooled (ZFC) and field-cooled (FC) processes with a 0.01 T applied field are shown in Fig. 5. The FC magnetization shows a continuous increase upon lowering the temperature, thus showing non-interacting or weak interacting particles.[21] The ZFC magnetization bifurcates from the FC process and shows a sharp and narrow peak at around 18 K, where the peak temperature $T_{\rm f} \approx 18$ K can be referred to as the average freezing temperature of the system. A similar result was also reported by Zysler *et al.*[14] To further study the magnetic transition, we measure the ac susceptibility $\chi_{\rm ac}$ of the NiO nanocrystal in the 5–80 K range at 0.1 kHz, 1 kHz, and 10 kHz (see the inset of Fig. 5). We can see a pronounced peak around

22 K. A careful investigation of $\chi'(T)$ reveals that with the rise in driving frequency (from 0.1 kHz to 10 kHz), the peak intensity decreases, and a small shift of peak position towards higher temperatures takes place. Such a frequency dependence of χ_{ac} is commonly observed in spin-glass systems.[22] In the present system, the asymmetric atomic arrangement and the broken exchange bonds of the magnetic cations in the layer disordered structure will lead to competing interactions between the randomly oriented spins. These competing interactions are known to cause spin frustration and consequently the SGL phase.[23] Thus, the SGL phase can exist in the layer disordered structure on the NiO surfaces, and the spin-glass transition observed in the ZFC curve should be the contribution of the surfaces.

The nanosized NiO with a surface SGL shell coupled with the inner AFM core has a natural structure for EB generation. In this paper, the EB effect is studied by measuring the magnetic hysteresis loops at 10 K after both ZFC and FC from 350 K under a cooling magnetic field of 2 T. As shown in Fig. 6, it can be seen that the hysteresis loop keeps a good central symmetry in the ZFC process but displays a negative exchange bias field (H_{EB}) $H_{EB} \approx 550$ Oe and a coercivity enhancement $\Delta H_C \approx 95$ Oe in the FC process. The H_{EB} is generally defined as $H_{EB} = -(H_1+H_2)/2$, where H_1 and H_2 are the left and the right coercive fields, respectively. Additionally, the system also exhibits a positive vertical magnetization shift $M_{shift} \approx 0.053$ emu/g, where M_{shift} is the difference in saturation magnetization between the measured loop and the loop centered in the M axis.

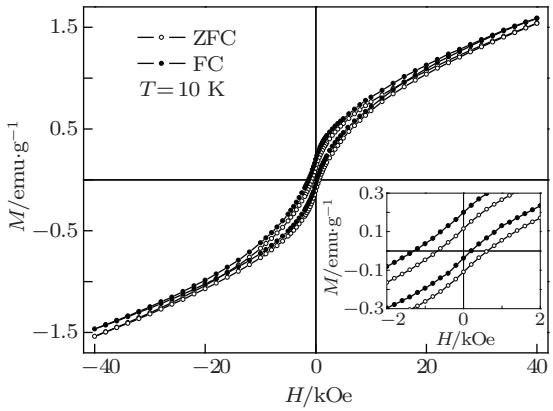


Fig. 6. ZFC and FC hysteresis loops measured at 10 K. The FC is under a magnetic field of 2 T from 350 K. The inset shows an enlarged view of the central part.

Nanoparticles can usually be considered to be composed of two parts. The inner part is the core, and the outer part is the shell. It has been revealed that for the NiO nanocrystals, the surface layers prefer to be SGL due to spin frustration. In order to generate the EB effect, the system must contain at least two exchange-coupled phases:[2] a reversible phase whose magnetic moment can be reversed, and a fixed phase whose moment cannot be reversed during the hysteresis loop measurements. As pointed out by Nogués *et al.*,[2] the SGL surface layer acts as FM on the AFM nanoparticle. Therefore, the SGL phase in the shell is the reversible phase; the AFM core is the fixed phase. When the sample is cooled down from 350 K to 10 K under an applied magnetic field, the moments in the shell line up with the field, and the spins next to the AFM core arrange along a specific direction due to the exchange interaction at the interface. Then the AFM spins at the interface exert a microscopic torque on the spins in the shell to keep them in their original direction during the magnetic field reversal. Thus, the magnetization loop is shifted to the opposite field axis, and a horizontal EB occurs. On the other hand, the opposite field can only reverse part of the SGL spins, the rest of the SGL spins stay frozen, which will show up as a vertical magnetization shift.

4. Conclusion

In this paper, monodisperse NiO nanocrystals with an average particle diameter of 3±0.4 nm are successfully synthesized by a modified thermal decomposition route, and this is confirmed by the excellent correlation among the XRD, TEM, HRTEM, SAED, and XPS data. The resulting material exhibits an SGL behavior at low temperatures due to the existence of a magnetically disordered surface shell. Moreover, the magnetic hysteresis loop shifts toward both the horizontal and the vertical directions at 10 K after field cooling. The observed EB effect is attributed to the exchange coupling between the AFM core and the SGL shell.

References

[1] Berkowitz A E and Takano K 1999 *J. Magn. Magn. Mater.* **200** 552

[2] Nogués J, Sort J, Langlais V, Skumryev V, Surinach S, Munoz J S and Baro M D 2005 *Phys. Rep.* **422** 65

[3] Xu X Y, Wang M H and Hu J G 2008 *Chin. Phys.* B **17** 1443

[4] Xu M, Pan J, Shen Y and Hu J G 2010 *Acta Phys. Sin.* **59** 7357 (in Chinese)
[5] Lü Q R, Fang Q Q and Liu Y M 2011 *Acta Phys. Sin.* **60** 047501 (in Chinese)
[6] Meiklejohn W H and Bean C P 1956 *Phys. Rev.* **102** 1413
[7] Yi J B, Ding J, Zhao Z L and Liu B H 2005 *J. Appl. Phys.* **97** 10K306
[8] Kavich D W, Dickerson J H, Mahajan S V, Hasan S A and Park J H 2008 *Phys. Rev.* B **78** 174414
[9] Tian Z M, Chen J T, Yuan S L, Tang J B, Huo S X and Duan H N 2011 *J. Appl. Phys.* **110** 053907
[10] Skumryev V, Stoyanov S, Zhang Y, Hadjipanayis G, Givord D and Nogués J 2003 *Nature* **423** 850
[11] Kodama R H and Berkowitz A E 1996 *Phys. Rev. Lett.* **77** 394
[12] Kodama R H, Makhlouf S A and Berkowitz A E 1997 *Phys. Rev. Lett.* **79** 1393
[13] Song X F and Gao L 2008 *J. Phys. Chem.* C **112** 15299
[14] Zysler R D, Winkler E, Mansilla M V and Fiorani D 2006 *Physica* B **384** 277
[15] Xia X H, Tu J P, Zhang J, Wang X L, Zhang W K and Huang H 2008 *Sol. Energy Mater. Sol. Cells* **92** 628
[16] Lee C Y, Chiang C M, Wang Y H and Ma R H 2007 *Sens. Actuators* B *Chem.* **122** 503
[17] Liu L, Li Y, Yuan S M, Ge M, Ren M M, Sun C S and Zhou Z 2010 *J. Phys. Chem.* C **114** 251
[18] Park J, Kang E, Son S U, Park H M, Lee M K, Kim J, Kim K W, Noh H J, Park J H, Bae C J, Park J G and Hyeon T 2005 *Adv. Mater.* **17** 429
[19] Tian Z M, Yuan S L, Yin S Y, Liu L, He J H, Duan H N, Li P and Wang C H 2008 *Appl. Phys. Lett.* **93** 222505
[20] Wertheim G K and Hüfner S 1972 *Phys. Rev. Lett.* **28** 1028
[21] Meneses C T, Duque J G S, Biasi E D, Nunes W C, Sharma S K and Knobel M 2010 *J. Appl. Phys.* **108** 013909
[22] Dho J, Kim W S and Hur N H 2002 *Phys. Rev. Lett.* **89** 027202
[23] Gruyters M 2005 *Phys. Rev. Lett.* **95** 077204